RECENT RESEARCH DEVELOPMENTS IN BELT CONVEYOR TECHNOLOGY

A.W. Roberts[1] and A. Harrison[2]

1. Dean, Faculty of Engineering, University of Newcastle, Australia.
2. Principal Research Scientist, Division of Applied Physics, CSIRO, Australia.

ABSTRACT

This paper outlines recent research in the area of belt conveying highlighting the research being conducted in Australia. A review of design trends associated with long overland conveyors is presented indicating the influence of economic and technical considerations in the design methodology. Aspects of conveyor dynamics are discussed and research and development work concerned with specific subjects including belt drum friction, rolling resistance and bulk solid and conveyor belt interaction. A test rig for examining stability between bulk solids and conveyor belts during transportation is described.

1. INTRODUCTION

Throughout the world bulk materials handling operations perform a key function in a great number and variety of industries. While the nature of the handling tasks and scale of operations vary from one industry to another and, on the international scene, from one country to another according to the industrial and economic base, the relative costs of storing and transporting bulk materials are, in the majority of cases, quite significant. It is important, therefore, that handling systems be designed and operated with a view to achieving maximum efficiency and reliability.

The theme embodied in the foregoing remarks is of direct relevance to Australia in view of the heavy dependence on bulk solids handling operations. While these operations range across the broad spectrum of the bulk handling field, a major emphasis is on the storage, handling and transportation of coal, mineral ores and agricultural products, notably grain, in large tonnages. An indication of the tonnages of principal minerals produced in Australia is given in Table I, while Table II summarises the mineral exports. Export earnings from minerals and agriculture are very substantial, with those from minerals approximating 50% and agriculture 30%.

Of the various modes of conveying bulk solids, belt conveyors are of considerable importance in view of their widespread use and proven reliability. Although their use is largely confined to in-plant movement of materials, their application to long distance overland transportation and to the conveying of large tonnages is gaining considerable interest. These applications are made possible through the development of steel cord conveyor belting with much potential seen in the newer light weight, high strength belt materials such as those reinforced with Aramid fibres.

Despite these developments, belt conveyor systems are often designed using static type analysis based on manufacturers' handbooks or current design standards. In general, steady state operation is assumed and belt tensions are computed on the basis of the drive requirements and the need to limit belt sag. High factors-of-safety of the order of 7:1 are adopted to account for unknown dynamic effects and uncertain belt splice efficiencies.

Fortunately, this situation is changing. Over recent years, significant improvements in conveyor

belt technology have occurred and more exacting design analysis procedures have arisen as a result of the considerable research that has taken place. There is now a much better understanding of the dynamic behaviour of belts during starting and stopping, as well as during operation, and this has led to resonance free designs, lower factors-of-safety and increased reliability.

In view of the importance of belt conveying to Australia's mining and mineral processing industries, it is not surprising that the subject of belt conveying has received considerable attention in terms of research and development. There has been wide acceptance by industry of the advances being made and this is reflected in the new conveyor installations particularly in regard to those associated with long overland transportation. The following list highlights some recent and current advances:

(i)   Conveyor dynamics – starting and stopping characteristics and dynamic belt stresses.

(ii)   Transverse vibrations of conveyor belts and the associated influence of idler spacing and troughing configurations on such vibrations.

(iii)   Conveyor belt idler resistance taking into account belt rubber hardness, sag, troughing configuration, idler/belt indentation and ambient operating temperature.

(iv)   Conveyor transition geometry.

(v)   Stability of bulk solid on conveyor belts during motion on horizontal and vertical curves.

(vi)   Conveyor belt/drive drum friction taking into account rubber hardness, surface roughness wrap angle.

(vii)   Steel cord splice design and analysis.

(viii) Conveyor belt monitoring as applied to steel cord and fabric belts

(ix)   Belt rip detection employing ultra sonic devices.

(xi)   Belt tension monitoring during operation.

(xii)   Belt cleaning including carry back measurement and development of improved cleaning efficiencies.

(xiii) Economic analysis applied to conveyor design.

A selection of research publications concerned with belt conveyor developments in Australia are given by References [1-26]. While it is beyond the scope of this paper to discuss these developments in any detail, an overview of some salient aspects of the research is presented.

TABLE I

PRODUCTION OF SELECTED MINERALS IN AUSTRALIA

(Monthly summary of statistics Australia - January, 1988)

Mineral	Unit of Quantity	1984–85	1985–86	1986–87	1st Quarter 1987–88
Coal	'000t	145,173	163,669	182,255	39,406
Lignite	'000t	38,500	35,469	42,656	10,268
Iron Ore	'000t	91,441	97,660	96,770	26,670
Manganese	'000t	1,858	1,966	1,585	4,710
Bauxite	'000t	31,839	32,432	-	-
Aluminium	'000t	8,120	9,080	9,838	2,573
Ilmenite	'000t	1,264	1,272	-	-
Rutile	'000t	191	212	-	-
Zircon	'000t	452	476	-	-
Nickel	t	80,267	80,528	74,654	18,800
Tungsten	t	1,830	1,830	1,249	295
Gold	kg	48,853	64,780	-	-
Copper	t	251,782	241,706	239,803	56,388
Lead	t	480,175	469,637	438,249	133,939
Zinc	t	731,321	689,411	715,974	185,766
Tin	t	6,430	7,391	8,524	1,873

TABLE II

VALUE OF AUSTRALIAN EXPORTS OF PRINCIPAL MINERAL PRIMARY PRODUCTS – 1986

(Aust. Mineral Industry Quarterly, Vol. 39 (4), 1986)

Bulk Material	Unit of Quantity	Quantity	Value of f.o.b. ($'000)
Alumina	'000t	7,687	1,427,168
Coal	'000t	92,717	5,364,142
Copper	t	140,133	247,567
Diamonds	carat	3,376,323	38,561
Gold	kg	58,735	972,591
Iron Ore	'000t	79,678	1,937,705
Lead	t	412,213	361,122
Nickel	-	-	438,044
Rutile	t	229,665	116,412
Silver	kg	957,710	53,750
Tin	t	7,494	58,229
Tungsten	t	2,526	13,482
Zinc	t	661,823	488,720

2. TRENDS IN CONVEYOR DESIGN

Recent research has shown that belts ranging in widths from 800 to 1200 mm are the most suitable. In this way, belt tensions are kept to acceptable limits allowing longer, individual conveyor lengths to be realised for the given range of belt SR values commercially available. For large tonnages, the use of belts within the abovementioned range of widths, but running at higher speeds provides the best solution. While these trends are supported on the grounds of economics, they are also supported on technical grounds. With regard to belt speeds, the economic evaluations clearly highlight the advantages of employing speeds greater than 4 m/s where large tonnage throughputs are involved.

The foregoing observations may be demonstrated as follows.

2.1 Basic Design Considerstions

The application of "steady-state" design theory provides a useful basis for the study of the first order influences of such factors as belt width, strength rating, factor-of-safety and costs for particular conveying tasks. While the design equations and theory are well known and documented, for the purpose of the present discussion, it is useful to briefly review the basic procedures. Referring to Figure 1, the following basic design equations apply:
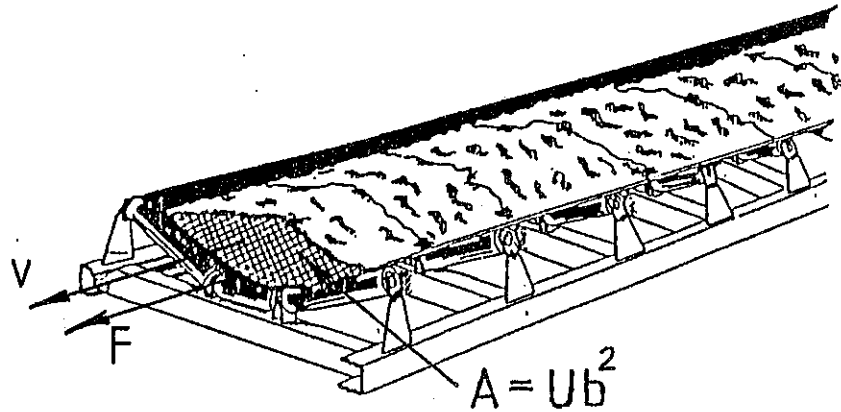
Figure 1   Conveyor Design Model

2.1.1 Throughput Q

$$Q = \rho A v \qquad (1)$$

where:

ρ — bulk density of bulk solid

v — belt velocity.

"A" represents the cross-sectional area of the bulk solid on the belt and is given by:

$$A = U b^2 \qquad (2)$$

where:

U — non-dimensional cross-sectional area shape factor

b — contact or "wetted" perimeter.

The belt width B > b to allow for edge effects.

Shape factors for various idler troughing configurations are given in Ref. [20].

2.1.2 Belt Resistance and Power

$$F = \sum_{i=1}^{n} F_i \qquad (3)$$

where F_i are the various resistances such as empty belt frictional resistance, load resistance, slope resistance, special and localised resistances such as those due to skirtplates and belt cleaners.

As a first order approximation, it may be assumed that the friction coefficients in the idlers and drive components are constant and independent of the velocity. It is then apparent that the total resistance to motion in functional form is:

$$F = f_1 (B, L \rho) \tag{4}$$

where:

B — belt width

L — total belt length.

The conveyor power is given by:

$$P = \frac{F v}{\eta} \tag{5}$$

where:

η — drive efficiency.

2.1.3 Peak Belt Tension

For a given arrangement, the tight side tension F_1 based on the simplified tension distribution around the drive drum(s) is given by:

$$F_1 = \left(\frac{e^{\mu\theta}}{e^{\mu\theta} - 1} \right) \tag{6}$$

This assumes the well known tension relationship

$$\frac{F_1}{F_2} = e^{\mu\theta} \tag{7}$$

where F_2 is "slack" side tension.

The maximum belt tension under steady-state operation will be the larger one of that given by Eq. (6) and that required to limit the maximum belt sag in the low tension zone of the belt. When dynamic effects are taken into account, the maximum belt tension will also include the influences of transverse and longitudinal belt vibrations. For a "first-order" approximation, it is clear that in functional form:

$$F_{max} = f_2 (B, L, \rho) \tag{8}$$

This equation indicates that the maximum belt tension for a given length conveyor is directly

related to the belt width. The narrower the belt, the lower the tension. However, the interrelation of belt width and conveyor speed needs to be taken into acocunt when establishing the most appropriate parameters to meet the throughput requirements.

2.1.4 Belt Rating and Width

For a computed maximum belt tension, the required belt width is given by:

$$B = \frac{F_{max}\, f_s}{SR} \qquad (9)$$

where:

f_s — factor-of-safety

SR— maximum strength rating of belt (in kN/m).

2.2 Conveyor Economic Analysis

Economic studies based on life-cycle cost analysis have been conducted to identify the most cost effective operating conditions for conveyors [1,10,20]. Relevant aspects of these studies are highlighted below. While the cost data are based on 1985 values, the relativity with respect to curret costs would be expected to be the same.

2.2.1 Belt Width and Velocity Considerations

Figures 2 and 3 show the annual equivalent costs per unit length for various throughputs for a conveying distance of 5 km. In Figure 2 the costs as a function of belt width are presented with belt velocities curves superimposed. The graphs show that the lowest costs occur in the range of belt widths 0.6 to 1.2 m with 1m being a 'good' average value. In Figure 3 the cost data are plotted as a function of belt velocity with belt width curves superimposed. As indicated, the annual equivalent cost decreases significantly at low belt velocities but, as the velocities increase, the cost is substantially constant or increases very slightly.
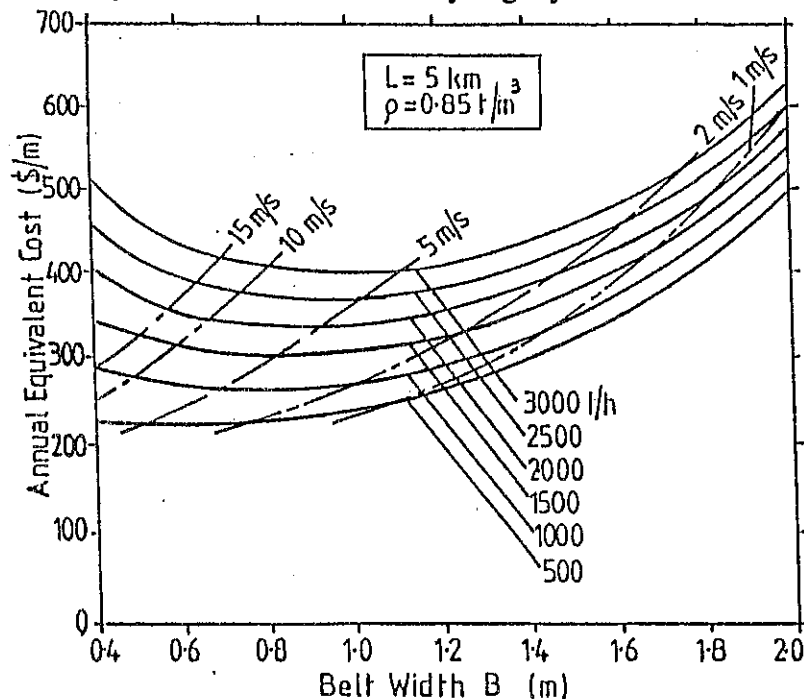

Figure 2. Annual equivalent cost per unit length as function of belt width
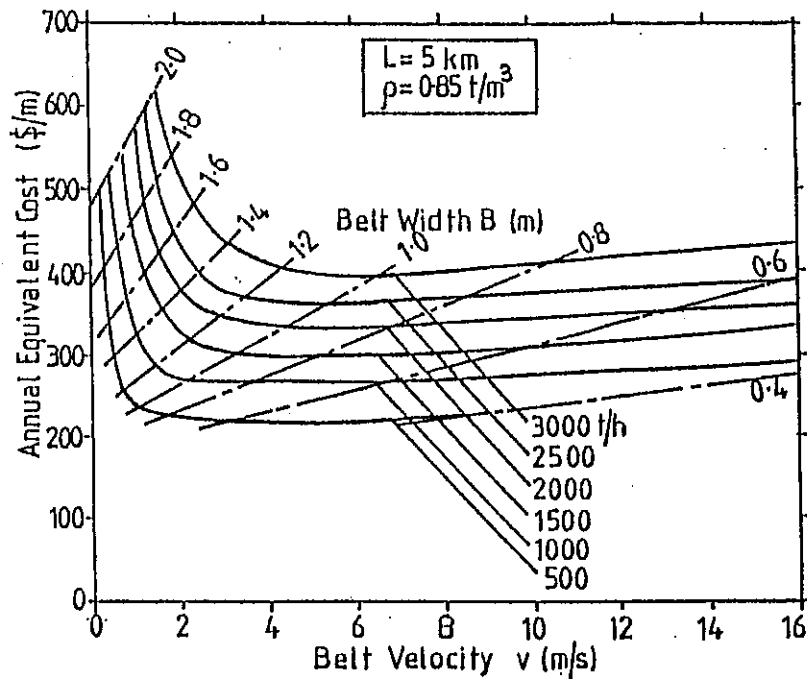
$$L = 5\ km,\ \rho = 0.85\ t/m^3,\ f_s = 7{:}1$$

Figure 3   Annual equivalent cost per unit length as function of belt velocity

$$L = 5 \text{ km}, \quad \rho = 0.85 \text{ t/m}^3, \quad f_s = 7{:}1.$$

2.2.2 Belt Length Considerations

The potential of belt conveyors for long distance transportation is illustrated in Figure 4. Here the annual equivalent cost per unit length is plotted as a function of conveyor length for various belt widths. The corresponding conveying velocities are indicated and the belt **SR** curves are superimposed.
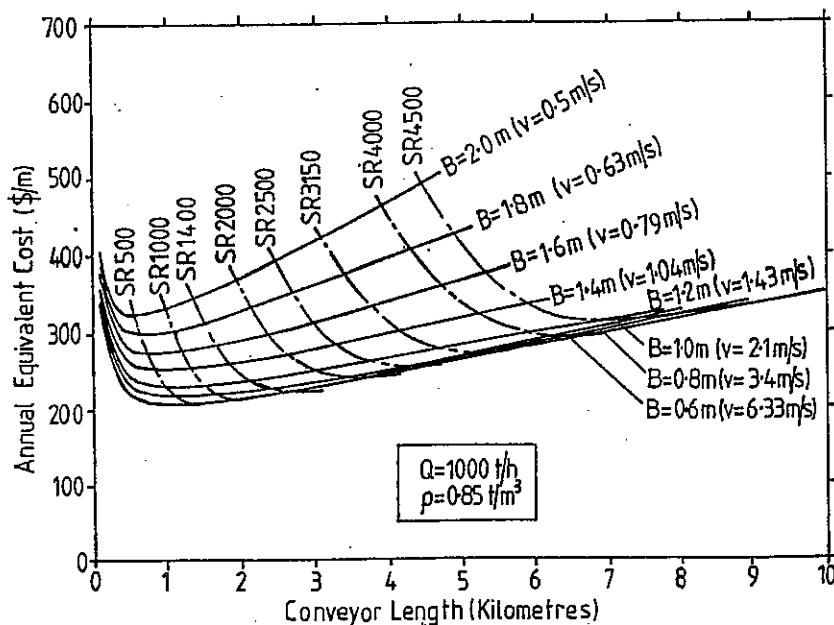

Figure 4   Annual equivalent cost per unit length for horizontal steel cord
Belt Conveyors. $Q = 1000$ t/h, $\rho = 0.85$ t/m^3

For conveyor lengths beyond 1 km, the cost per unit length increases as shown, this being due to the need to employ belts with higher **SR** values. For this reason it would be nominally more economical to use several shorter conveyors in series than fewer longer conveyors for conveying over long distances. This could well be the case when wide belts are used. However, the cost per unit length advantages associated with shorter belts would be offset by the cost of the transfer stations. Hence it is recommended that, in general, longer individual belts be used and this reinforces the need to employ narrower belts.

2.3   Dynamic Considerations

The two most important dynamic considerations in the design of belt conveyors are:

(i)   Reduction of starting and stopping stresses in the belt.

(ii)   Running stability or resonance-free operation.

2.3.1 Dynamic Belt Stresses – Starting and Stopping of Conveyors

Numerous methods have been devised for starting belt conveyors, including eddy current drives, switched resistance starts, fluid and fluid-scoop coupling drives and controlled starting for AC and DC motors. Most of these methods have discontinuities in the drive acceleration at the instant torque is applied to the belt, leading to travelling elastic waves in the belt [4]. Measurement of starting tensions in belts containing shock waves indicates that tensions in the belt may exceed ten times the highest operating tension, and this has been the reason for the high safety factors that have been adopted in the past. Large safety factors increase the cost of belting manufacture.

The control of belt speed during the start-up and running period is most important in higher speed belts if shock is to be avoided and if lower belt safety factor "sf" is to be employed to reduce installation and driving costs. During the braking period, similar considerations apply; however, the concept of emergency stopping must be reviewed when belt speed is increased. Naturally, all safety requirements must be much more closely observed near the running belt and at the loading and discharge stations.

The criteria for minimising transient stresses in conveyor belts during starting and stopping particularly applies to fast belts. The dynamics of starting and stopping have been examined in some detail by Harrison [5]. He showed that an optimal "stop start" is given by the belt start-up velocity.

$$v(t) = \frac{v_b}{2} \left(1 - \frac{\pi t}{T} \right) \quad \text{for} \quad t < T$$

$$= v_b \quad \text{for} \quad t > T \tag{10}$$

where:

v_b — belt running velocity

T   — run-up period.

The form of Eq. (10) is shown in Figure 5. With modern computer control systems, it is possible to generate the desired starting characteristic.

$$V(t) = \frac{V_b}{2}(1 - \cos\frac{\pi t}{T}) \; ; \; t \leq T$$
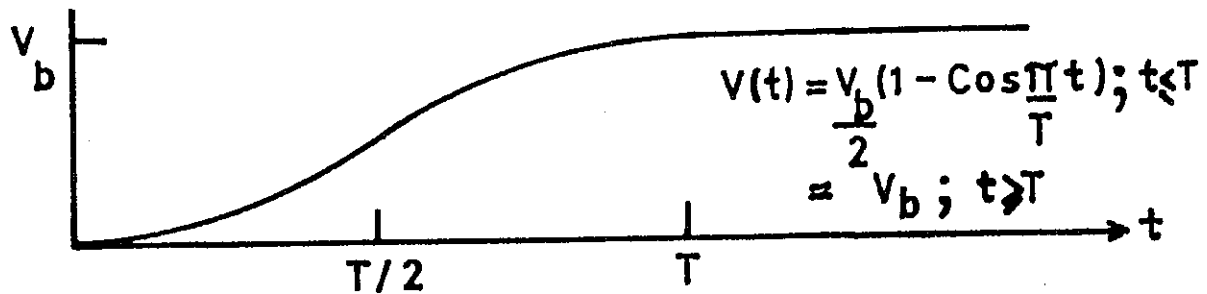$$\approx V_b \; ; \; t \geq T$$

Figure 5. Ideal belt velocity characteristic to minimise transient tensions at start and stop

A general formula for the factor-of-safety has been proposed.

$$\text{f.o.s.} \geq 3 \left(1 + \frac{T_d}{T_{max}} + \frac{\Sigma_a T_a}{T_{max}} \right) \qquad (11)$$

where T_d is the non-oscillatory dynamic belt tension during transient periods, ΣT_a are additional tensions due to transitions, impact and vertical curves. The peak tension T_{max} along the belt is determined from conventional design methods such as DIN 22101 or ISO 5048.

It needs to be noted that the above expression is somewhat idealised inasmuch as many other factors need to be taken into account. These factors include splice efficiency, belt quality and tracking characteristics.

2.3.2 Conveyor Design Program

A dynamic analysis program shown in Figure 6 uses the results of conventional handbook procedures and modifys the design in the light of computed dynamic stresses.

The value of T_d critically depends on the starting or stopping characteristic of the motor drive or brake. An over-rated belt is progressively de-rated in this programme until a suitable f.o.s. is achieved. Typically a f.o.s. ≥ 3.3 is obtained and the belt strength and hence cost is significantly reduced. In the case where a steel cord belt is selected, the weight is reduced in the selection process, leading to further reductions in tension and power.

The design cost is computed each time the static design is modified in the programme loop. Though the flowchart of Figure 6 does not show a different path for calculating f.o.s. for starting or stopping, the largest average acceleration in the transient period should also give the largest dynamic acceleration in the belt. As a result, the greatest rate-of-change of belt velocity must be employed in f.o.s. calculations.
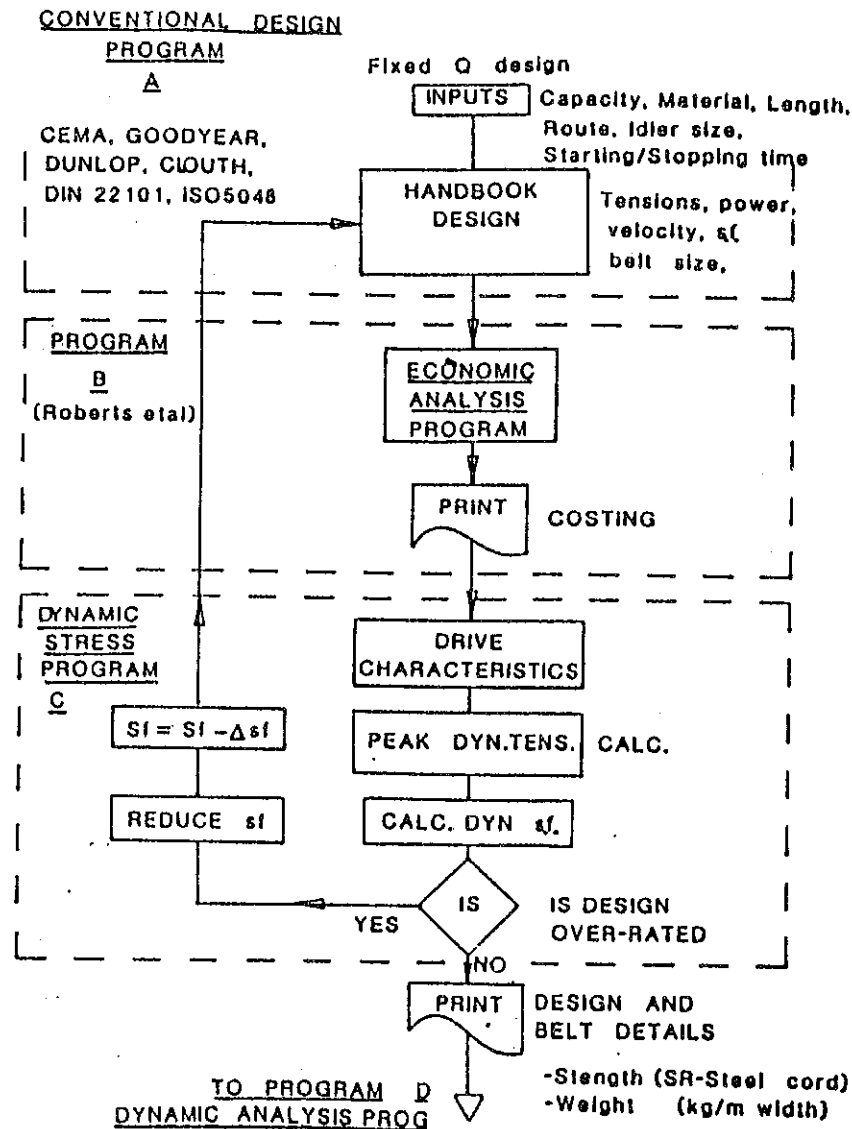
Figure 6. Dynamic analysis flowchart for evaluating the starting and stopping safety factors in conveyor belts, in conjunction with conventional design

2.3.3 Resonance Free Design

Elimination of belt resonances by the correct design of idler spacing, belt tensions and belt weight will result in lower operating costs due to increased idler life and reduced belt failure caused by vibration of the belt.

Variables that are available for design optimisation are the excitation frequency of the idlers f_i and the belt modal frequency f_{mn} [2,3]. The condition for stable belt running is expressed by the relation

$$\Sigma_q \{(qf_{mn} + \Delta f_{mn}) < f_i < (qf_{mn} - \Delta f_{mn})\} \quad q = 1,2,.... \quad (12)$$

where f_{mn} is the natural frequency of the tensioned belt. Plate mechanics [5] are used to determine these frequencies.

Figure 7 illustrates the application of Eq. (12), and shows the location of idler frequency in relation to belt frequency.
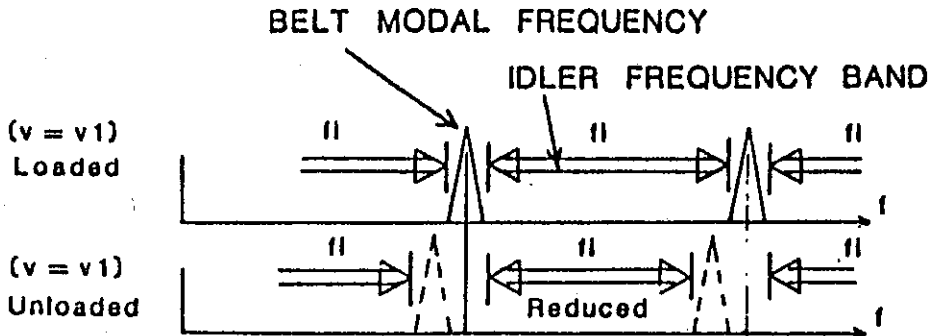

Figure 7. Change of modal frequencies for a belt due to tension variation between loaded and unloaded conditions

The running belt tension profile is required in order to design idler diameter d, idler spacing a, belt width b and belt speed, so that $f_i < f_{mn}$ or a multiple of this frequency in the case of multi-lobed idler eccentricities. Usually only single lobe idler eccentricities occur in manufacture.Conventional static design, as distinct from dynamic design, only uses loading, tension and belt sag (including takeup counterweight masses) to obtain idler spacing.

In dynamic design, the belt width is selected and then f_{mn} and f_i are calculated. The belt speed and idler diameter, together with belt width and throughput, are adjusted and the dynamic design is repeated until $f_i < f_{11}$ and the design is complete. The belt frequencies are determined for both loaded and unloaded conditions to obtain design ranges. Generally, for very high-speed designs near 15 ms^{-1}, belt width is b ~ 0.8 m, a ~ 2 m and idler diameters are d ~ 0.20 m.

It should be be appreciated that while the power requirement to drive a belt increases with belt speed, high speed belts are obviously narrow to prevent resonances, and so rolling losses are less with narrow belts in a linear proportion to the width. However, belting and structure cost is considerably reduced in narrow belt systems and so long-distance high speed narrow belts are more economical. Figure 8 shows how transverse belt resonances may be eliminated by idler spacing considerations between loaded and unloaded conditions.
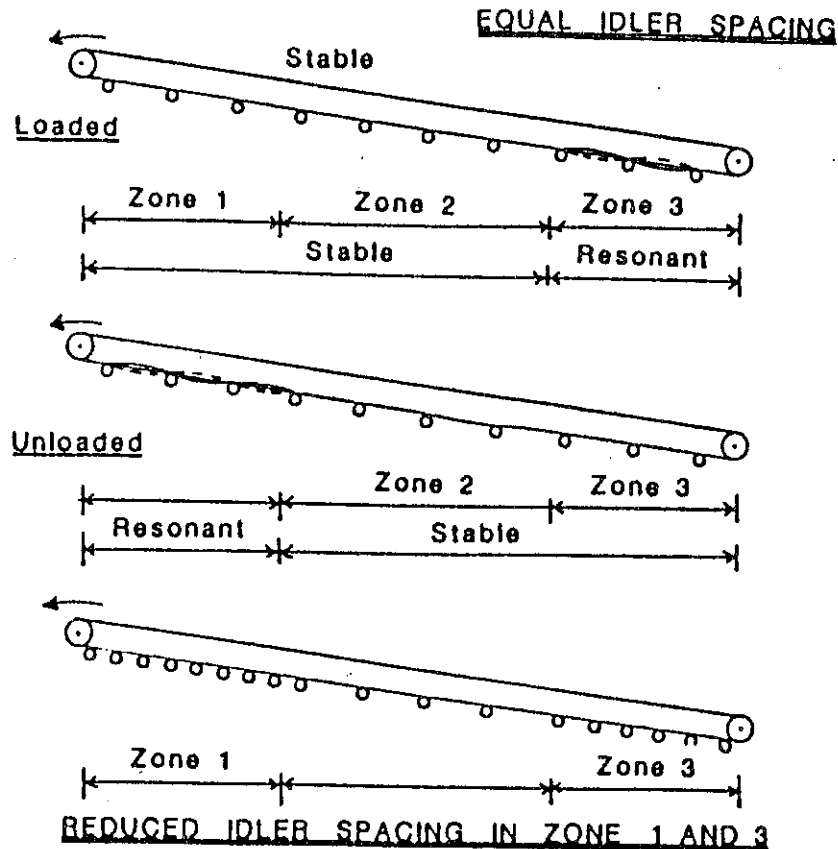
Figure 8   Diagram showing the removal of resonance zones by the application of change of idler spacing in the resonance zone

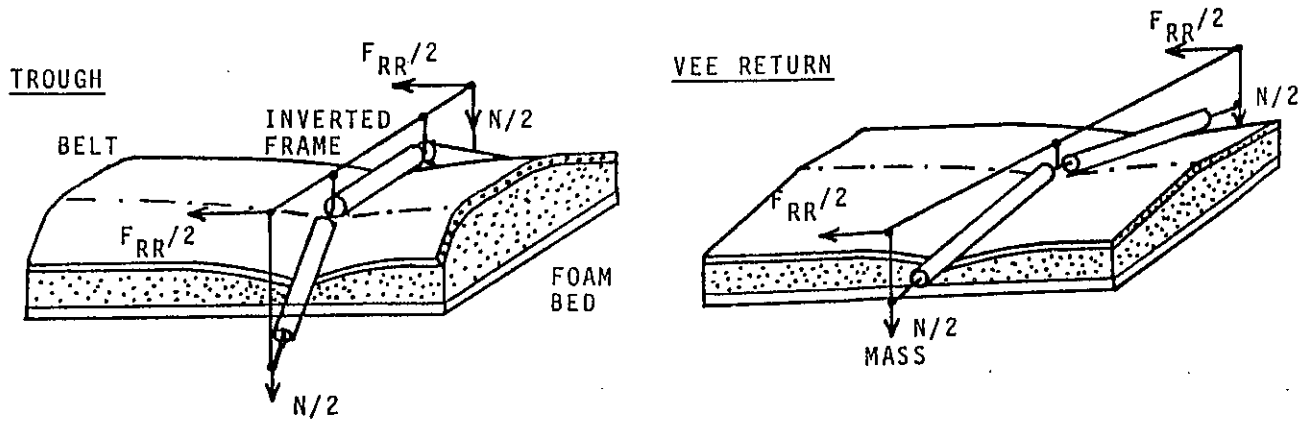## 4.   BELT IDLER RESISTANCE AND IDLE BEARING PERFORMANCE

4.1   Idler Resistance

The determination of idler resistance has been based, traditionally, on the application of "artificial friction" coefficients which are quite empirical. More recently, research has been undertaken to examine the nature of belt and idler rolling resistance from a more fundamental viewpoint. This is of particular importance in the case of long overland conveyors where the cumulative influence of idler resistance demands an accurate determination of the individual resistance contributions.
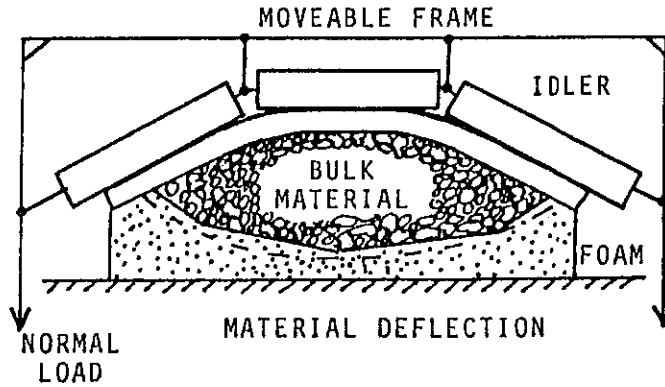
One study performed by Harrison et al [14] has examined the various factors influencing idler resistance. Factors taken into account are:

(i)   Belt sag

(ii)   Idler diameter

(iii)   Indentation effects

(iv)   Belt hardness

(v)   Temperature

(vi)   Idler configuration.

The simulation test rig, constructed for this purpose, is shown in Figure 9.

(a) Apparatus for Testing Empty Belts in their Operating Shapes

(b) Test Set-Up for Loaded Belt

Figure 9.   Simulation Test Rig for Measurement of Idler Resistance

Experiments have shown that the idler resistance is somewhat insensitive to idler diameter;   all other parameters have an influence.

The total resistance due to the carry idlers has been shown to be

$$F_{RC} = \left(\mu_i + \mu_s + \mu_f \right) N + F_{BC} \qquad (13)$$

where:

μ_i =   indentation coefficient depending on rubber hardness

μ_s =   sag coefficient

μ_f =   flexure coefficient

F_{BC} =   bearing losses of carry side idlers

N =   normal load on idler set.

The components of the total resistance are defined below:

$$\mu_i = 0.022 - \frac{0.0113}{32} \left(H - 55 \right) \qquad (14)$$

An appropriate linear expression for the hardness H as a function of temperature is

$$H(T) = 0.5\,T + 80 \qquad (15)$$

where:
H = Hardness — Shore A degrees
T = Temperature °C.

The belt sag friction factors μ_s for steel cord, fabric and PVC belts are 0.0033, 0.0066 and 0.005 respectively, for a belt sag of 1%. The sag friction along the whole return conveyor from head $(n = 0)$ to tail $(x = \ell)$, is computed using

$$\mu_s(x) = \mu_s \left[1 - \frac{x}{L} \right]^{-1} A \qquad (16)$$

where

$$A = \frac{\mu_0}{\mu_s} \qquad L = \frac{\ell}{B} \qquad B = (1 - A)$$

An average value of the sag for the whole length of the conveyor is $\mu_{s/2}$.
Experimentally the combined friction coefficient

$$\mu_{isf} = \mu_i + \mu_s + \mu_f \qquad (17)$$

has been measured. The flexure coefficient μ_f has been measured indirectly by this approach. It is obtained by subtracting $(\mu_i + \mu_s)$ from μ_{isf}.

3.2 Idler Bearing Life

The rolling fatigue life of a properly lubricated bearing is expressed in terms of the B-10 life rating. For a sample of nominally identical bearings, the B-10 life, expressed in millions of revolutions at constant speed or hours of operation, is the life that 90% of the bearings in the sample will attain or exceed before the first signs of fatigue are evident. The B-10 life is expressed by:

$$L_{B-10} = \frac{10^6}{60\,n} \left(\frac{C}{P} \right)^u \qquad (18)$$

where:

n — rotational speed (in rev/min)

C — basic dynamic load rating (as given in bearing catalog)

P — actual bearing load

u — u = 3.0 for bass bearings, u = 3.33 for roller bearings.

(The load units for C and P are the same.)

It is evident from Eq. (16) that, in the case of idler bearings for belt conveyors, the life is inversely proportional to the belt speed. However, as indicated by Talks and Kenny [27] of the National Coal Board (NCB), U.K., the limiting factor for idler life is the grease life rather than the B-10

fatigue life. For instance, Talks and Kenny estimated that the NCB has around 11×10^6 idler bearings in operation at any one time with load ratios C/P ranging from 13.8 to 41.9; the corresponding B-10 lives range from twelve years to 360 years, based on continuous running at 400 rev/min. Yet, the average grease life for idler bearings is five years for operation at 50°C and two years at 70°C.

Much progress is being made to extend idler bearing life, and the work reported by Herraty and Bras [28] concerning a SKF seize resistant bearing is worth noting. The seize resistant bearing was compared, under dry abrasive test conditions, with three other bearings, a standard deep groove ball bearing (DGBB), a DGBB with increased clearance and a taper roller bearing. The results are shown in Table 3. As indicated, the seize resistant bearings had a B-10 life ten times that of the DGBB with increased clearance, 15.6 times that of the standard DGBB and 70 times that of the tapered roller bearing. The mean power consumption during all tests showed the seize resistant bearing to have the lowest power, being 64% of that for the standard DGBB, 78% of that for the DGBB with increased clearance and 46% of that for the tapered bearing. The test failure mode for the seize resistant bearing was by eventual wear without seizure, whereas the other three bearings all failed by seizure.

A more recent paper by Herraty and Hamblin [29] has reported on the service life calculations of idler bearings. Continued testing of the seize resistant bearing has confirmed the superiority of this type of bearing under arduous operating conditions in dirty environments.

TABLE 3

COMPARISON OF BEARING PERFORMANCE -

DRY ABRASIVE TEST CONDITIONS

(Ref. Herraty and Bras [28])

Bearing Type	L_{B-10} Life Revolutions	Test Failure Mode	Mean Power Consumption (w)
Seize Resistant (SKF 420205)	1.40×10^6	Wear	28.0
Standard DGBB (SKF 6205)	0.09×10^6	Seizure	44.0
DGBB-increased Clearance (SKF 6205-64)	0.14×10^6	Seizure	35.7
Taper Roller LM11949/LM11910	0.02×10^6	Seizure	61.0

4. CONVEYOR BELT AND DRIVE DRUM INTERACTION

4.1 Introductory Remarks.

An important aspect of belt conveyor operation is the frictional resistance generated between the belt and drive drum. The resistance controls the development of drive tensions. In accordance with Figure 10, the well known tension relationship (referred to in Section 2.1.3), which is widely used in design, is

$$\frac{F_1}{F_2} = e^{\mu \theta} \tag{19}$$

where F_1 = Tight side tension

F_2 = Slack side tension

θ = wrap angle

μ = coefficient of friction between belt and drum

It is usual to assume that $\mu = 0.25$ to 0.3 for a steel drum surface and $\mu = 0.35$ for a lagged drum surface. The principal assumptions embodied in equation (19) are:

(i) the frictional resistance is strictly of Coulomb type

(ii) the friction is developed around the contact surface of the drive drum

(iii) slip (or pending slip) occurs around the contact surface

(iv) eccentricity of the surface defining cord location (and hence tensions) and drum surface is neglected

These assumptions are not strictly valid and values normally assigned to μ in equation (19) are not actual friction coefficients but, rather, empirical values which are lower in magnitude than the actual values. Although it is never stated, the reduced empirical friction coefficients used in equation (19) provide for a conservative design; they compensate for the fact that unless slip occurs around the contact surface, the friction may not be fully developed.
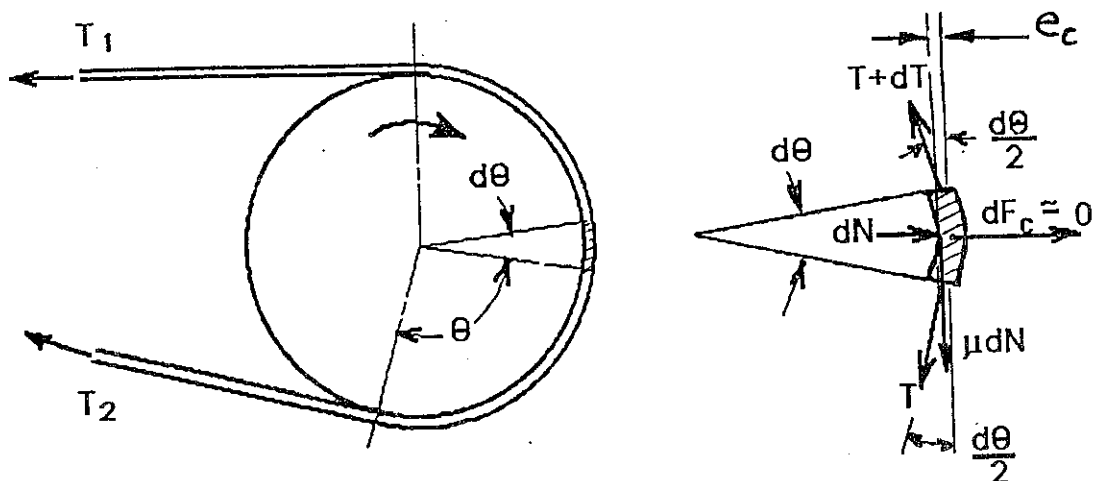

Figure 10. Tensions Generated on Drive Drum

It is quite clear that the eccentricity "e_c" in Figure 10 causes internal shear to be developed in the rubber as a result of the moment generated. It is also known that the angle of wrap may be divided into combinations of active slip, creep and passive zones as depicted in Figure 11. This causes variations in the tensions as indicated.
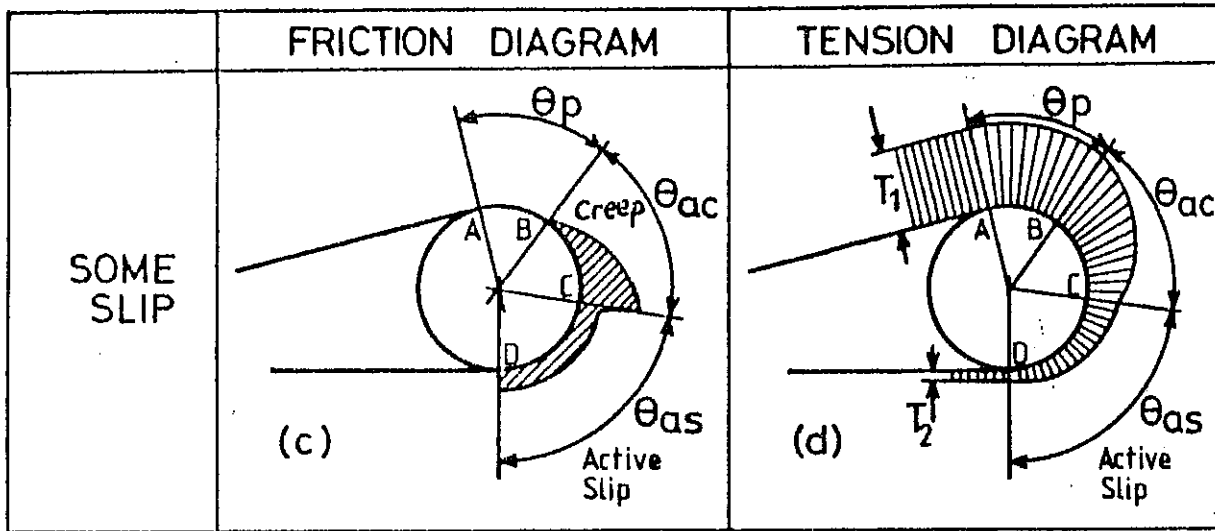
	FRICTION DIAGRAM	TENSION DIAGRAM
SOME SLIP		

Figure 11 Typical Belt Friction and Tension Diagram for Combinations
of Slip, Creep and Passive Zones.

4.2   Current Research

A program of research being conducted at the University of Newcastle is aimed at providing a greater insight into belt and drive drum friction [21]. To date, the research has involved experimental studies using two separate test set-ups.

(i)   Direct Shear Apparatus   (Figure 12)

(ii)   Drum Friction Apparatus   (Figure 13)

The Direct Shear Apparatus of Figure 12 is based on the Jenike Direct Shear Tester. For a range of belt and drum samples records of shear load and shear deformation were obtained for a range of normal loads. By way of example, the fully developed friction for steel on rubber has been shown to depend on the surface roughnesses of the belt and steel surfaces and, in particular, on the rubber hardness.
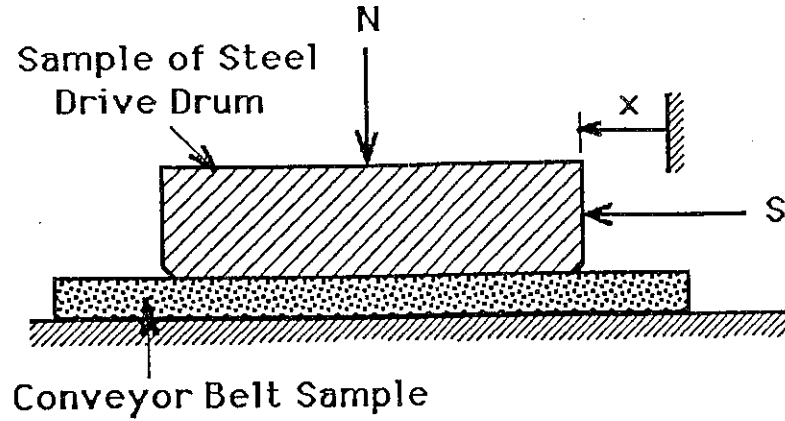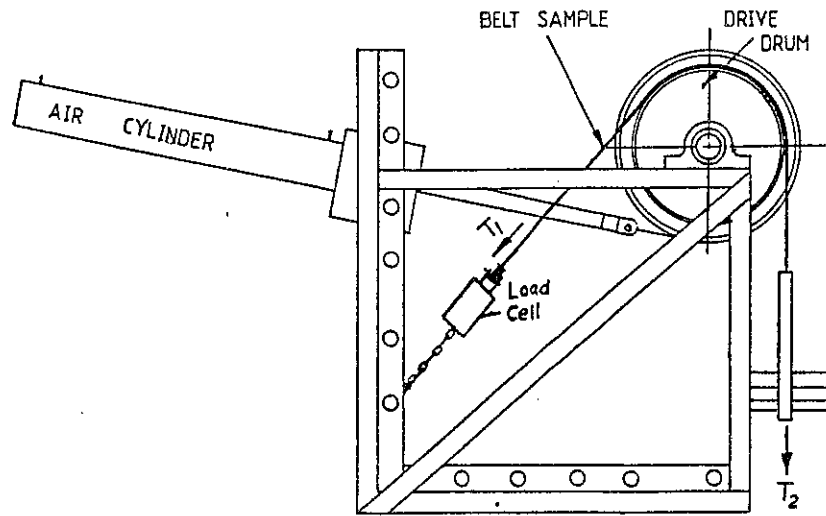
Figure 12. Direct Shear Tests

Figure 13 Drum Friction Apparatus

Tests have shown that the fully developed friction is given by

$$\mu = \frac{C_o}{2 R_a} \exp [\frac{H - H_o}{C_1 R_a}] + \mu_o \qquad (20)$$

where

$$\mu_o = C_2 R_a^2 + C_3 R_a + C_4 \qquad (21)$$

where $H_o = 66$ $C_o = 1.0$ $C_1 = 10$

$C_2 = -2.9$ $C_3 = 4.37$ $C_4 = -0.8$

R_a = Roughness of steel drum

The influence of rubber hardness is illustrated in Figure 14 which shows the comparison between the measured and predicted values of the friction coefficient; the predicted values are based on equation (20).
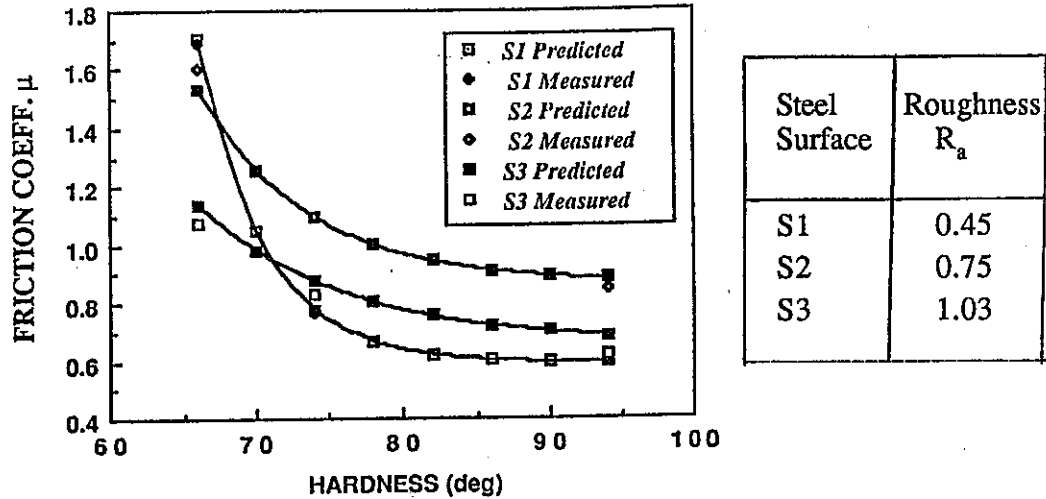

Steel Surface	Roughness R_a
S1	0.45
S2	0.75
S3	1.03

Figure 14. Comparison Between Predicted and Experimental
Results for three Steel Surfaces S_1, S_2, S_3

The influence of wrap angle has been examined using the drum friction apparatus of Figure 13. Preliminary results indicate that the tension relationship does not follow the exponential form of equation (19); a linear relationship of the form given below has been indicated.

$$\frac{F_1}{F_2} = 1 + C\,\theta \qquad (22)$$

where C = Constant

On the basis of the above relationship, the equivalent friction decreases with wrap angle indicating that the friction coefficient is inversely proportional to the tension. However, these findings are somewhat tentative and further tests are necessary before any firm conclusions can be obtained. More recent experiments carried out over a wider range of wrap angles confirmed the general exponential form of equation (19) but with significantly higher values of the friction coefficient μ than those currently used in design. Current research is concentrating on finite element analyses of the stress conditions in belts wrapped around drive drums; the results are expected to provide greater insight into the fundamental nature of belt and drum friction.

5. BULK SOLID AND CONVEYOR BELT INTERACTIONS

It is important that, during the design stage, careful consideration be given to the interaction between the conveyor belt and the bulk solid being conveyed. Interaction effects relate to such aspects of conveyor operation as the stability of the bulk solid during transportation and the discharge characteristics. The latter concerns the design of the discharge chute and the belt cleaning system.

5.1 Stability of Bulk Solid on Belt During Conveying

The loading of bulk solids onto conveyor belts is governed by the need to ensure effective transport of a maximum payload without spillage. This requirement becomes particularly important in the

case of long, overland conveyors which execute a combination of vertical and horizontal curves.

In order to gain some insight into the load stability during transportation, a conveyor simulation test rig was designed and constructed at the University of Newcastle, Australia [24]. The test rig, which is illustrated in Figure 15, comprises three main components:

    (i)   Conveyor belt clamping and tensioning mechanism;

    (ii)   Cam driven troughing idler unit to simulate the belt and material passing over consecutive idler sets; and

    (iii) Main support frame incorporating a two-way tilting base to accommodate vertical inclines and/or the superelevation of horizontally curved conveyor belts.
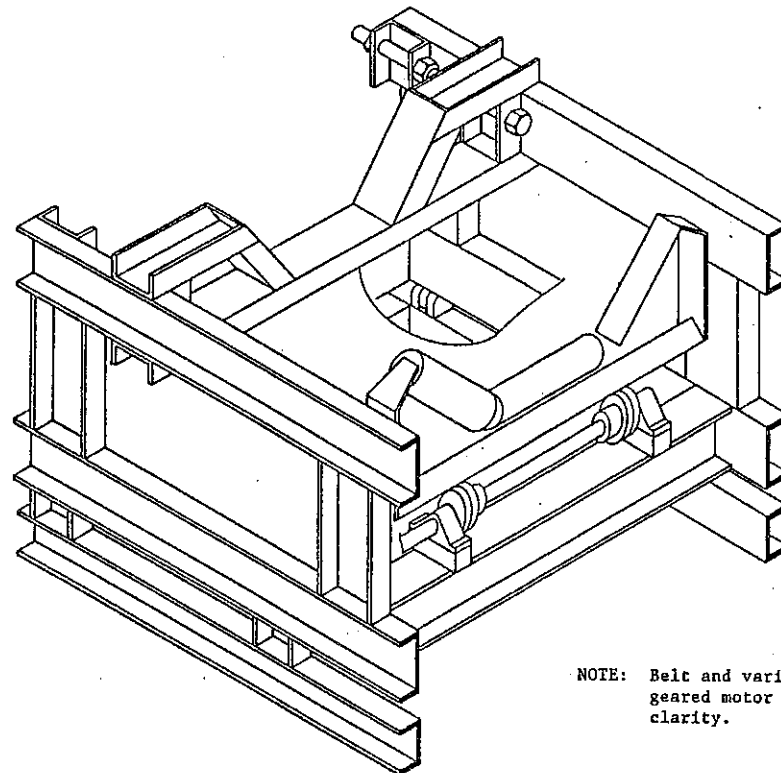

NOTE: Belt and variable speed geared motor omitted for clarity.

Figure 15. Schematic isometric drawing of the conveyor simulation test rig

6.1.1 General Specifications

The general specifications of the test rig are:

    (i)   All belt types with belt widths up to 1050 mm;

    (ii)   Carry idlers to any diameter and specification. Idler types include flat carry idlers, 3 roll in-line and offset troughing idlers (20, 30, 35 and 45°), and 3 roll and 5 roll suyspended troughing idlers. Idler spacing is varfiable from 1000 - 2000 mm.

    (iii) Simulated belt speeds ranging from 0 - 15 m/s are possible via a 3ph A.C. geared motor unit fed by a variable frequency electronic drive.

    (iv) Belt sag and/or belt tension is controlled through two hydraulic jacking cylinders. The cylinders allow the belt to be adjusted to a present tension, or until a required percentage sag (either for coasting or loaded) is achieved.

(v) Frequency and amplitude of belt vibration is to simulate material on an actual belt passing from a position on top of an idler set down to the maximum sag position (midway between consecutive idler sets) and finally to the top of the next idler set.

The cam drive which controls the amplitude of vibration is adjusted so that the loaded belt moves between the maximum sag position to level with the belt clamping and tensioning brackets (that is, the top of the next idler set). The frequency of vibration is set to the idler passing frequency which is a function of belt speed and idler spacing.

Although the rig does not currently allow the idler rotating frequency to be superimposed it is believed that whilst the frequencies are higher, the amplitudes are so small that the effect of the rotating idlers will be negligible compared to the idler passing motion described above.

5.1.2 Typical Test Results

A range of tests have been conducted over a period of time to simulate the motion of bulk materials, notably coal and iron ore. In the case of the latter, one series of tests was concerned with the stability of iron ore on the horizontally curved section of an overland conveyor. By way of illustration, a typical set of results are shown in Figure 16.

The results relate to a 35 deg. idler set, the conveyor rig being set at a horizontal curve super-elevation angle of 8 deg. The iron ore was at a moisture content 0.8% (wet basis) and of a particle size of 90% minus 16 mm. As the results show, there was very little movement of the iron ore.
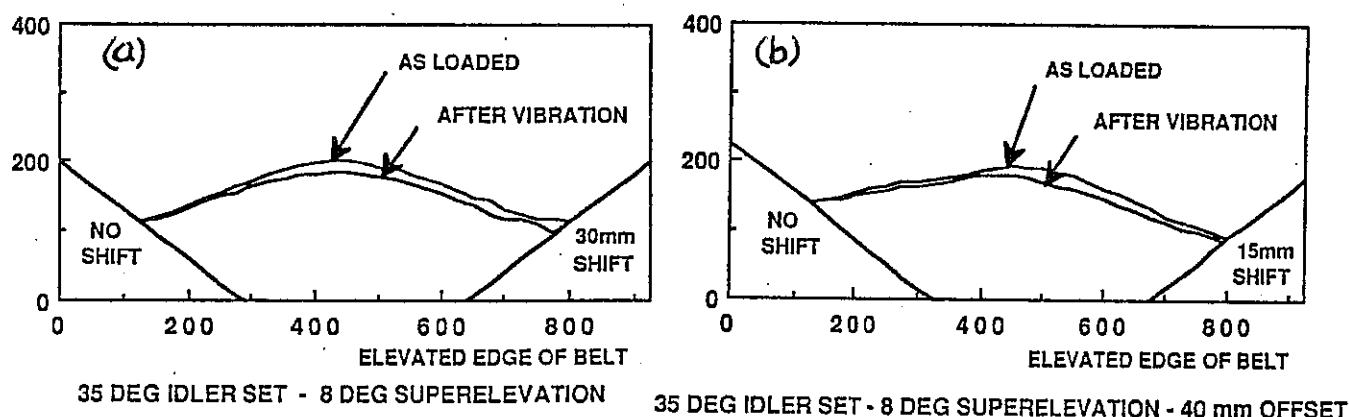

Figure 16. Change in surcharge profile between 'as loaded' and after prolonged simulated motion for

(a) Horizontally curved conveyor at a superelevation angle of 8° with symmetrically positioned belt on 35° troughing idlers.

(b) Horizontally curved conveyor at a superelevation angle of 8° with the belt offset 40° mm down the 35° troughing idlers.

5.2 Bulk Solid Discharge and Carry-Back After Discharge

5.2.1 Condition Occurring at Discharge

An indication of the discharge trajectories and possible levels of bulk solid carry-over following discharge may be ascertained by considering, in a simplistic way, the mechanics of separation of bulk solids from the belt as it passes around the discharge pulley [13,19]. Figure 17 shows the condition at the conveyor discharge.

The equilibrium condition for the position at which discharge commences is given by

$$\frac{v^2}{r\,g} = \cos\theta + \frac{\sigma_o}{\rho\,g\,h} \tag{23}$$

where v = velocity of bulk solid leaving belt (m/s)
      r = radius of bulk solid measured from drum centre (m)
      g = gravitational acceleration
      θ = angle at which discharge commences
      σ_o = adhesive stress (kPa)

      ρ = bulk density (t/m^3)
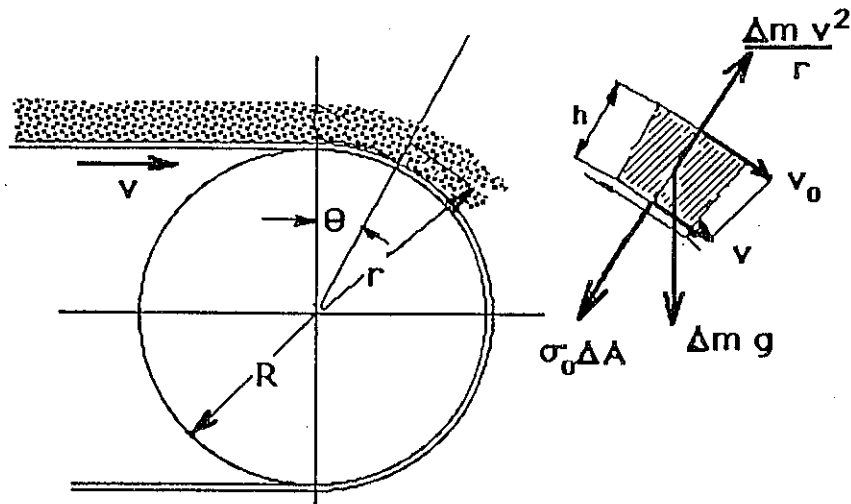   h = thickness of bulk solid stream (m)

Figure 17 Conveyor Belt Discharge

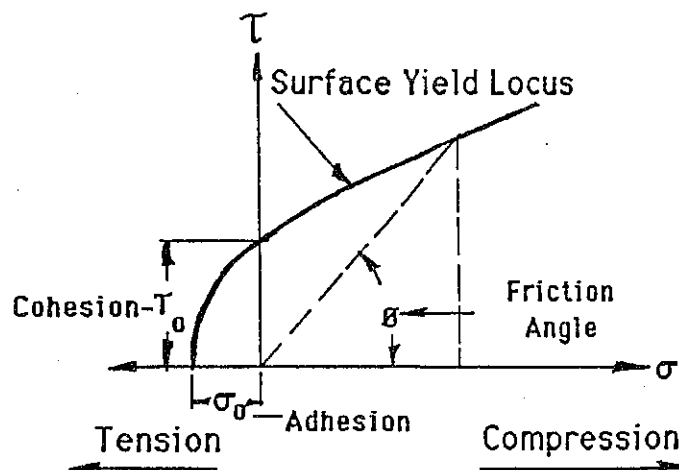The adhesive stress, depicted in Figure 18, is obtained from the Surface Yield Locus measured in the laboratory.

Figure 18. Surface Yield Locus for Conveyor Belt

Referring to Figure 19, the average height of material on the belt is given by

$$h = \frac{Q}{\rho \, v \, b} \qquad (24)$$

where Q = throughput (t/h)
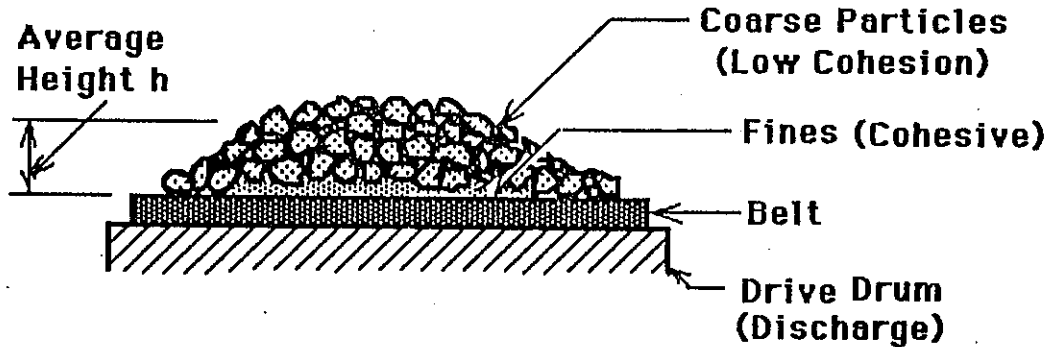 b = width of contact of bulk solid on belt (m)

Figure 19. Bulk Material on Belt at Discharge

Discharge will commence at the line of intersection of the belt and drive drum, that is, for $\theta = 0$. The minimum belt velocity for this to occur follows directly from (23) and is given by:

$$v_{min} = \sqrt{\frac{r \, \sigma_o}{\rho \, h}} \qquad (25)$$

By way of example, consider the belt conveying of bauxite. While the bulk density varies with the consolidation pressure, it is assumed that $\rho = 1.2$ t/m^3 corresponding to the likely consolidation condition (from flow property data). Measurements of surface yield loci of bauxite indicate that adhesive stresses up to 1 kPa may occur. Assuming a value of h = 0.09 (m) and a radius of R = 0.6 m, then

$v_{min} = 2.35$ m/s

Hence, if the belt speed $v \geq 2.35$ m/s, then discharge will commence at the line of intersection of the belt with the drum.

5.2.2. Carry-Over After Discharge

Referring to Figure 20, assuming the bulk solid does not slide relative to the belt, discharge takes place as discussed previously. For cohesive bulk solids, sliding is unlikely in view of the very high friction angle that accompanies the low normal pressures between the bulk solid and the belt.
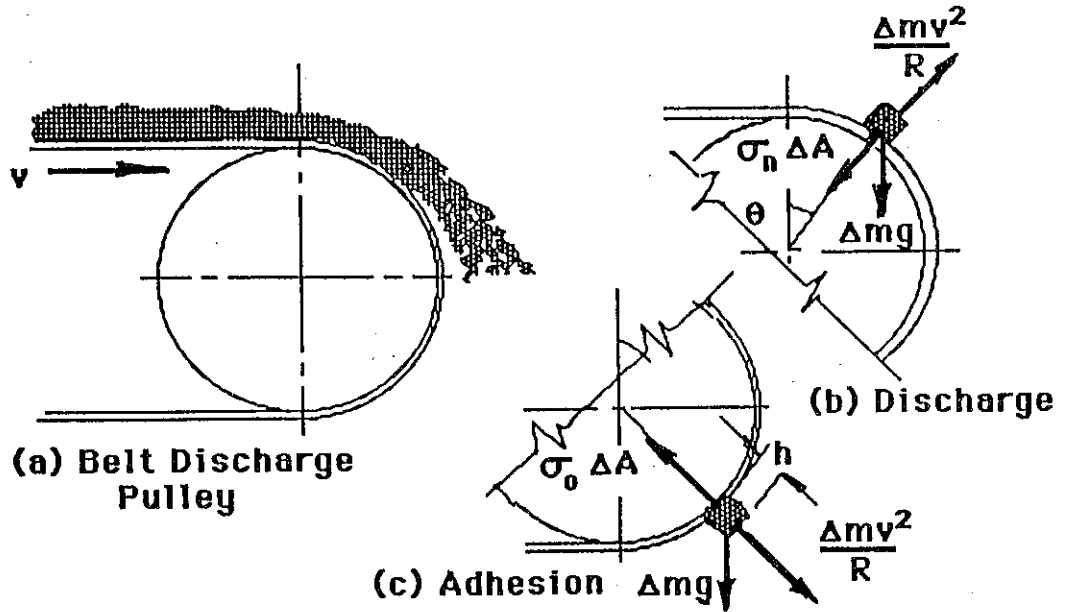
Figure 20. Mechanics of Discharge and Adhesion

After the point of discharge defined by equation (23), some bulk solid will adhere to the belt as carry-over. This is an adhesive condition that arises as a result of negative or tensile stresses σ_{nt} which occur between the bulk solid and the belt surface, as indicated in Figure 18. While these stresses are very small, they can have a significant influence on the amount of carry-over that may occur. An indication of the thickness h of the carry-over may be obtained as follows:

For an arbitrary location defined by $\theta > \theta_L$, where θ_L where is the angle at which discharge commences, it follows that the thickness h of the carry-over is given by

$$h = \frac{\sigma_{nt}}{\rho} \left[\frac{1000}{\dfrac{v^2}{R} - g\cos\theta} \right] \qquad (26)$$

where h = carry over on belt (mm)

   σ_{nt} = tensile stress (kPa)

   ρ = bulk density (t/m³)
   v = belt velocity (m/s)
   R = pulley radius (m)
   g = gravitational acceleration.

The critical location occurs when $\theta = 180°$, that is at the bottom of the pulley. For this location $\sigma_{nt} = \sigma_o$ (see Figure 18); the thickness h is given by

$$h = \frac{\sigma_o}{\rho} \left[\frac{1000}{\frac{v^2}{R} + g} \right] \qquad (27)$$

By way of illustration, values of σ_o as high as 1.4 kPa for iron ore at 11% moisture content on conveyor belt surfaces have been measured. It is usual for values lower than this to occur.

Assuming, for example, that $\sigma_o = 0.1$ kPa and density $\rho = 1$ t/m^3, then $\sigma_o/\rho = 0.1$. From the foregoing, it follows that for a belt travelling at 3 m/s and assuming a 1 metre diameter discharge pulley, bulk solid will adhere to the belt in thicknesses up to $h = 3.6$ mm. Values such as this give an indication of the amount of bulk solid to be handled by a belt cleaner.
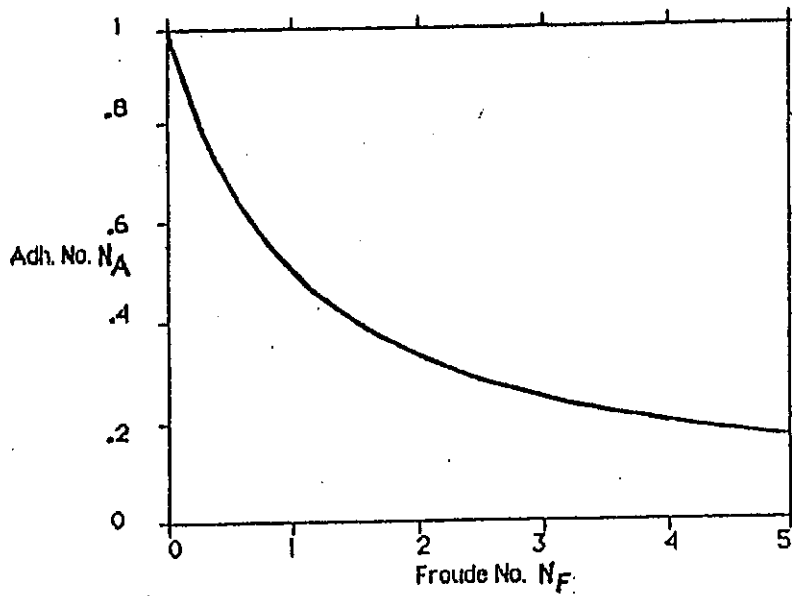

Figure 21. Belt Carry-Over at Discharge Pulley Expressed in Non-Dimensional Form

The carry-over analysis may be generalised by presenting the parameters in non-dimensional form. From equation (27) it follows that

$$N_A = \frac{1}{N_F + 1} \qquad (28)$$

where

$$N_A = \frac{\rho \, g \, h}{\sigma_o} = \text{Adhesion Number} \qquad (29)$$

$$N_F = \frac{v^2}{R \, g} = \text{Froude Number} \qquad (30)$$

The relationship between N_A and N_F is shown in Figure 21.

5.2.3 Belt Cleaner Operation

Effective belt cleaning depends on an appreciation, at the design stage, of the amount of likely carry-over of bulk material after discharge. It is unlikely that a single cleaning device will be sufficient and a multiple cleaner system is recommended.

Apart from the selection of the most appropriate cleaning device, it is important that sufficient attention be given to the need to ensure effective removal of bulk material without build-up on the cleaner components. As illustrated in Figure 22, build up can occur on bolt projections and ledges, thus impairing the performance of the cleaner. Such projections should be avoided.
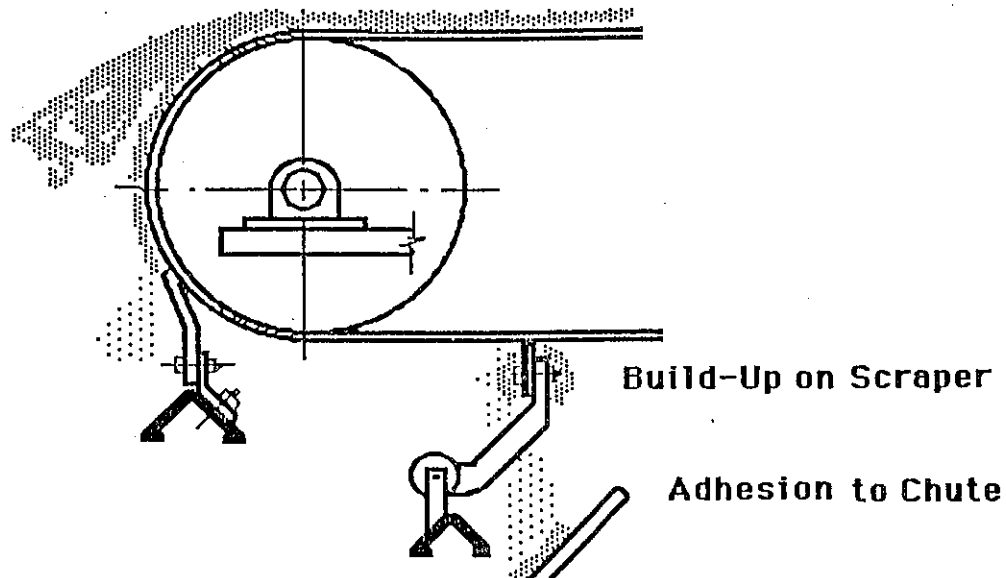

Build-Up on Scraper

Adhesion to Chute

Figure 22. Belt Cleaner System Showing Areas of Possible Build-Up

6. OTHER RESEARCH DEVELOPMENTS

While it is beyond the scope of this paper to discuss, in any detail, other areas of research, it is of interest to note areas in which research is research is presently being conducted.

6.1 Belt Tracking and Dynamic Tensions

Two of the more important parameters needed by the designer of belt systems are the dynamic tracking characteristics and dynamic belt tensions that occur on starting and stopping. Both of these parameters are difficult to predict during the design phase. There are no theories to predict belt tracking characteristics based on belting construction, particularly with a bonded steel cord belt in which cord load sharing is not always uniform. Research being conducted by Harrison [22] is addressing this problem. A dynamic sag measuring transducer has been developed and monitoring of belt tracking and sag during starting and stopping has provided new ways of proving that these parameters have significant importance. The tracking and dynamic characteristics may be predicted in advance during belt manufacture.

6.2 On Line Control of Belt Dynamics

Using the sag transducer mentioned in 6.1 above, Harrison has provided a methodology for the on line control of conveyor belt dynamic characteristics [24]. The analysis takes into account the design and location of belt tensioning devices.

6.3 Conveyor Belt Monitoring

Following the development of the steel cord belt monitor [5], a fabric belt monitor has been developed by Harrison [17]. This device employs non-contact capacitive transducers and can readily detect cuts in the cover material, edge damage, repairs, splices and a number of manufacturing defects. The monitor is shown schematically in Figure 23. The monitoring device has scope for introduction into manufacturing processes in order to provide improved quality assurance.
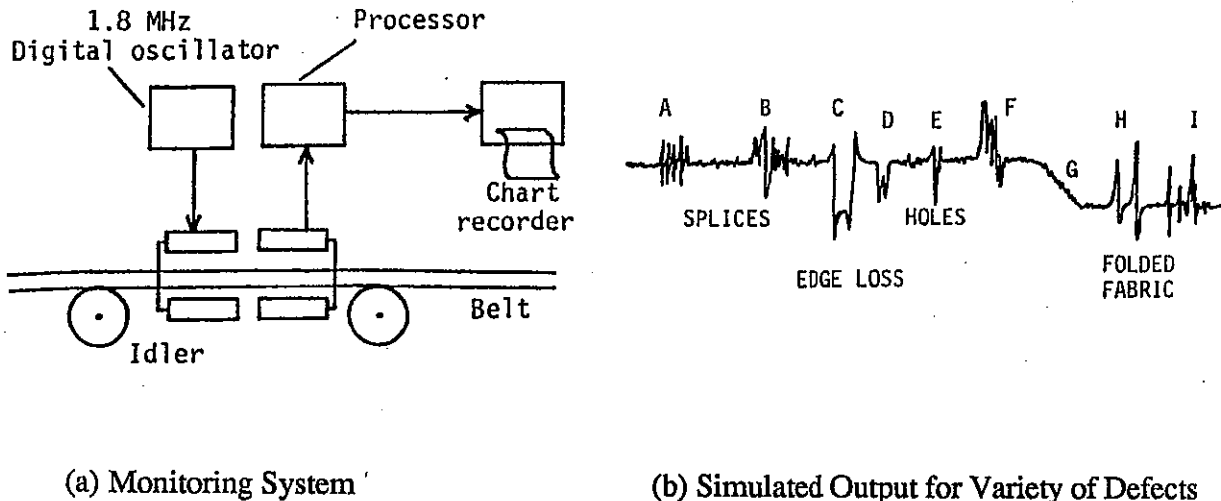
(a) Monitoring System

(b) Simulated Output for Variety of Defects

Figure 23. Monitoring System for Fabric Belts

6.4 Use of 'Kevlar' Aramid Fibres in Conveyor Belts

Research at the University of Newcastle by Betz et al [11,18] has concentrated on the improvement of splices in 'Kevlar' reinforced belts. Various splice configurations have been examined and it has been shown that splice strengths greater than the parent belt are possible. Two and three dimensional finite element models have been developed to analyse the stress distributions in splices.

7. CONCLUDING REMARKS

It is clear that significant developments are continuing to be been made in the field of belt conveying. Like other countries in the world dependent on bulk materials handling, Australia has been active in research and development work in the various facets of bulk handling, including belt conveying. Some of the developments that have occurred in recent years in Australia have been highlighted in this paper. It is particularly gratifying to note the wide industrial acceptance of modern design methods and monitoring procedures. The interaction between industry and research institutions is of great importance in guiding current research and indicating new research directions.

8. REFERENCES

1. Roberts, A.W., Hayes, J.W. and Scott, O.J.,"Optimum Design of Continuous Conveyors". Bulk Solids Handling, Vol. 1, No. 2, 1981.

2. Harrison, A., "Flexural Behaviour of Tensioned Conveyor Belts", Mech.Eng.Trans. IE(Aust.), Vol. ME8 (1983), No. 3.

3. Harrison, A. and Roberts, A.W., "Technical Requirements for Operating Conveyor Belts at High Speed", Bulk Solids Handing, Vol. 4 (1984), No. 1, pp.99-104.

4. Harrison, A., "Criteria for Minimising Transient Stress in Conveyor Belts", Mech.Eng.Trans IE(Aust), Vol. ME8 (1983), No. 3, pp.129-134.

5. Harrison, A, "Dynamic Measurement and Analysis of Steel Cord Conveyor Belts", Ph.D. Thesis, The University of Newcastle, Australia, March, 1984.

6. Harrison, A. and Roberts, A.W., "Future Design of Belt Conveyors Using Dynamic Analysis". Paper presented at Transportation 1984, IE(Aust).

7. Roberts, A.W. and Hayes, J.W., "Economic Analysis in the Optimum Design of Conveyors", TUNRA, The University of Newcastle, Australia, 2nd Ed., 1980,. ISBN 0-7259-3406.

8. Roberts, A.W., Hayes, J.W. and Scott, O.J., "Optimum Design of Continuous Conveyors", Bulk Solids Handling, Vol. 1 (1981), No. 2, pp.255-264.

9. Harrison, A., Hayes, J.W. and Roberts, A.W., "The Feasibility of High Speed Narrow Belt Conveying for Bulk Solids Handling:, Mech. Eng. Trans. IE(Aust.), Vol. ME7, (1982), No. 3.

10. Roberts, A.W., Harrison, A. and Hayes, J.W., "Economic Factors Relating to the Design of Belt Conveyors for Long Distance Transportation of Bulk Solids", Int. Jnl. of Bulk Solids Handling, Vol. 5, No. 6, December 1985 (pp.1143-1149).

11. Betz, E., "The Use of 'Kevlar' Aramid Fibres in Conveyor Belts, Part 1: Pull-Out Problem and Splice Design", Intl. Jnl of Bulk Solids Handling, Vol. 6, No. 2, 1986 (pp.355-367).

12. Harrison, A., "Troughability Measurement of Fabric Reinforced Belting for the Powder and Bulk Handling Industry", Intl. Jnl. of Bulk Solids Handling, Vol. 7, No. 3, June 1987 (pp.381-384).

13. Roberts, A.W., Ooms, M. and Bennett, D.J., "Bulk Solid Conveyor Belt Interaction in Relation to Belt Cleaning", Intl. Jnl. of Bulk Solids Handling, Vol. 7, No. 3, June 1987 (pp.355-362).

14. Harrison, A., Teo, L.H. and Roberts, A.W., "Measurement of Belt-Idler Interactions and Material Flexure Coefficients for Design of Troughed Conveyor Systems", Intl. Jnl of Bulk Solids Handling, Vol. 7, No. 3, June 1987 (pp.367-371).

15. Harrison, A., "Future Design of Belt Conveyors Using Dynamic Analysis", Intl. Jnl. of Bulk Solids Handling, Vol. 7, No. 3, June 1987 (pp.375-379).

16. Attwood, R. and Smith, B.D., "Assessment of Air Velocity Profiles in Belt Conveyor Galleries and their Drying Effect on Brown Coal During Transportation", Intl. Jnl. of Bulk Solids Handling, Vol. 7, No. 3, June 1987 (pp.385-390).

17. Harrison, A., "A New Development in Textile Belt Monitoring", Intl. Jnl. of Bulk Solids Handling, Vol. 8, No. 2, April 1988 (pp.231-233).

18. Roberts, A.W., Betz, E., Goh, B.N., Law, S.C. and Wang, W.C., "The Use of 'Kevlar' Aramid Fibres in Conveyor Belts, Part II: Static Strength of Splices", Intl. Jnl. of Bulk Solids Handling, Vol. 8, No. 4, August 1988 (pp.429-441).

19.   Roberts, A.W. and Bennett, D.J., "Friction, Adhesion and Wear in Conveyor Belt Cleaning Operations", AntiWear 88, The Royal Society, London, 1988 (pp.28.1-28.8).

20.   Harrison, A. and Roberts, A.W., "Modern Concepts in Belt Conveying and Handling of Bulk Solids", TUNRA, The University of Newcastle, Australia, 1988.

21.   Roberts, A.W., Papaliski, D. and Harrison, A., "The Friction and Tension Characteristics on Driving Drums of Conveyor Belts", Proceedings, 12th Intl. Power and Bulk Solids Handling Conference, Chicago, U.S.A., May 1988.

22.   Harrison, A., "New Concepts for Evaluating Belt Tracking and Dynamic Tensions", Third Intl. Conf. on Bulk Materials, Storage, Handling and Transportation, IE(Aust), Newcastle, June 1989 (pp.114-118).

23.   Harrison, A. and Barfoot, G., "Modelling the Effect of Take-Up Location on Conveyor Belt Performance", Third Intl. Conf. on Bulk Materials, Storage, Handling and Transportation, IE(Aust), Newcastle, June 1989 (119-123).

24.   Bennett, D.J. and Roberts, A.W., "Bulk Solid and Conveyor Belt Interaction During Transportation", Third Intl. Conf. on Bulk Materials, Storage, Handling and Transportation, IE(Aust), Newcastle, June 1989 (pp.345-358).

25.   Harrison, A., "Stress Distribution in Steel Cord Belts with Cord Plane Defects and Inlaid Repairs", Intl. Jnl. of Bulk Solids Handling, Vol. 8, No. 4, Aug. 1988 (pp.443-446).

26.   Morrison, W.R.B., "Computer Graphics Techniques for Visualizing Belt Stress Waves", Intl. Jnl. of Bulk Solids Handling, Vol. 8, No. 2, April 1988 (pp.221-227).

27.   Talks, M.G. and Kenny, P., "The Evaluation of Some Fire-Resistant Greases as Lubricants for Conveyor Idler Bearings", Proc. Tribology in Mineral Extraction War on Wear Conf., Sept. 1984, I.Mech.E., University of Nottingham.

28.   Herraty, A.G., and Bras, J.C.M., "Rolling Bearings for Hostile Environments", Proc. Tribology in Mineral Extraction War on Wear Conf., Sept. 1984, I.Mech.E., University of Nottingham.

29   Herraty, B. and Hamblin, R.F., "Idler Rollers - Observations and Predictions", AntiWear 88, The Royal Society, London, 1988 (pp.27.1-27.8).